PHYSICAL REVIEW D **93,** 075035 (2016)

Probing $(g-2)_\mu$ at the LHC in the paradigm of *R*-parity violating MSSM

Amit Chakraborty* and Sabyasachi Chakraborty†

Department of Theoretical Physics, Tata Institute of Fundamental Research, 1, Homi Bhabha Road, Mumbai 400005, India

(Received 17 December 2015; published 27 April 2016)

The measurement of the anomalous magnetic moment of the muon exhibits a long-standing discrepancy compared to the standard model prediction. In this paper, we concentrate on this issue in the framework of the *R*-parity violating minimal supersymmetric standard model. Such a scenario provides a substantial contribution to the anomalous magnetic moment of the muon while satisfying constraints from low energy experimental observables as well as the neutrino mass. In addition, we point out that the implication of such operators satisfying muon $g-2$ are immense from the perspective of the LHC experiment, leading to a spectacular four muon final state. We propose an analysis in this particular channel which might help to settle the debate of *R*-parity violation as a probable explanation for $(g-2)_\mu$.

DOI: 10.1103/PhysRevD.93.075035

I. INTRODUCTION

We are living in an era enriched with many experimental breakthroughs and results. Recently, the two CERN based experiments, namely ATLAS and CMS collaborations, have confirmed the existence of a neutral boson, widely accepted to be the Higgs boson with mass close to 125 GeV [1]. All the decay modes of this scalar boson have been measured with moderate accuracy, and the results obtained so far are fairly consistent with the standard model (SM) expectation. However, from an aesthetic point of view, the SM inevitably has the hierarchy problem which is associated with the stabilization of the Higgs boson mass from large radiative corrections. Further, the observation of neutrino mass and mixing and the existence of dark matter (DM) most certainly require beyond the standard model (BSM) physics. Another sector which requires the intervention of BSM theories is the anomalous magnetic moment of the muon, quantified as $a_\mu = (g-2)_\mu/2$, which has been measured with unprecedented accuracy at the Brookhaven $(g-2)$ experiment. However, there still exists a discrepancy between the experimental observation and the SM prediction, given by $\Delta a_\mu = a_\mu^{\rm exp} - a_\mu^{\rm SM} = (29.3 \pm 9.0) \times 10^{-10}$ [2]. This anomaly with respect to the SM expectation reflects the contributions arising from the perturbative higher order electroweak (EW) corrections, the virtual hadronic inputs, and the possible presence of the BSM physics.

Supersymmetry (SUSY) [3–6] remains one of the most celebrated BSM theories till date. The minimal supersymmetric standard model (MSSM) provides an elegant solution to the hierarchy problem [4,6]. In addition, neutrino masses and DM can also be explained in the paradigm of MSSM. Another important feature of MSSM is that it yields a sizable contribution to the muon $(g-2)$ requiring light first two generation sleptons [7,8]. However, the ATLAS and CMS experiments, in their hunt for superpartners, have found no significant excess over the SM background after the $7+8$ TeV run of the LHC [9,10]. For comparable gluino and first two generation squark masses, the bound on these particles can be as large as 1.7 TeV in *R*-parity conserving (RPC) and simplified phenomenological MSSM scenarios [11]. On the other hand, the constraints on the first two generation sleptons are comparatively weaker and lie in the ballpark of 300 GeV [12,13]

In MSSM, the loop contributions to $(g-2)_\mu$ arise if there is a chirality transition in the external muon lines. This chirality transition requires an insertion of a fermion mass or a Yukawa coupling vertex. In the framework of *R*-parity conserving SUSY, the main possibilities for the chirality flip are the following: (a) a muon line through a muon mass term, which contributes to a factor m_μ; (b) a Yukawa coupling in between the Higgs field and μ_L, μ_R which contributes to a factor y_μ; (c) a *L*-*R* mixing in the scalar sector, more precisely corresponding to a transition between $\tilde{\mu}_L$-$\tilde{\mu}_R$, which contributes to a factor proportional to $m_\mu \mu \tan\beta$, where μ is the Higgsino mass parameter and $\tan\beta$ is the ratio of two vacuum expectation values v_u and v_d associated with the two Higgs doublets H_u and H_d, respectively. Finally (d) a SUSY Yukawa coupling of a Higgsino to muon and $\tilde{\mu}$ or $\tilde{\nu}_\mu$, contributing a factor of y_μ. It is evident that all of these contribute to the muon $(g-2)$ and an overall rough estimate implies $a_\mu \sim m_\mu^2/M_{\rm SUSY}^2$ [14]. Therefore, the new physics scale or more precisely the SUSY scale must be around $\mathcal{O}(100)$ GeV; i.e., the electroweak scale will have large contributions to $(g-2)_\mu$.

On the other hand, one of the many interesting outcomes of *R*-parity violating (RPV) MSSM [15] is that it is an intrinsic way by which substantial augmentation of muon

*amit@theory.tifr.res.in
†sabya@theory.tifr.res.in

$(g-2)$ can be obtained [16]. Further RPV is also interesting as it is an inherent SUSY way to generate neutrino masses both at the tree level and at the one loop level. In this work, we consider a RPV MSSM scenario with relevant operators, which can give a sizable contribution to the anomalous magnetic moment of the muons. We respect the collider bounds on the slepton masses as well as indirect constraints from neutrino masses and low energy observables to present a self-consistent picture. Most importantly, RPV MSSM also provides direct spectacular signals at the LHC. It is important to note that we ignore the contributions originating from left scalar and right scalar fermion mixing terms as they are negligible. There exist several phenomenological studies incorporating the muon $(g-2)$ anomaly and the LHC bounds in R-parity conserving and violating SUSY framework; a partial list can be seen in Refs. [17–26].

The plan of this paper is as follows. In Sec. II, we look into the theoretical framework of the study under consideration and its effects on $(g-2)_\mu$. In Sec. III, we study the relevant constraints coming from low energy observables and neutrino masses, which is necessary for considering a $\mathcal{O}(1)$ RPV coupling. Section IV is dedicated to a numerical analysis with appropriate benchmark points followed by a detailed discussion on the present bounds from LHC data. In Sec. V, we perform a dedicated collider analysis to correlate the fact that $(g-2)_\mu$ from the RPV MSSM scenario can leave its fingerprints in the LHC experiments. Concluding remarks and related discussions are relegated to Sec. VI.

II. MUON $(g-2)$ IN MSSM

When R-parity is conserved, the SUSY effects on a_μ include contributions from the chargino-muon sneutrino and neutralino-smuon loops. The generic expressions for one loop SUSY contributions to a_μ, including the effects of possible complex phases, are given as [27,28]

$$a_\mu^{\tilde{\chi}^0} = \frac{m_\mu}{16\pi^2}\sum_{i,m}\left\{-\frac{m_\mu}{12m^2_{\tilde{\mu}_m}}(|n^L_{im}|^2+|n^R_{im}|^2)F_1^N(x_{im}) + \frac{m_{\tilde{\chi}^0_i}}{3m^2_{\tilde{\mu}_m}}\mathrm{Re}(n^L_{im}n^R_{im})F_2^N(x_{im})\right\}, \quad (1)$$

$$a_\mu^{\tilde{\chi}^+} = \frac{m_\mu}{16\pi^2}\sum_{k}\left\{\frac{m_\mu}{12m^2_{\tilde{\nu}_\mu}}(|c^L_k|^2+|c^R_k|^2)F_1^C(x_k) + \frac{2m_{\tilde{\chi}^\pm_k}}{3m^2_{\tilde{\nu}_\mu}}\mathrm{Re}[c^L_k c^R_k]F_2^C(x_k)\right\}, \quad (2)$$

where $i=1,2,3,4$, $m=1,2$, and $k=1,2$ denote the neutralino, smuon, and chargino mass eigenstates, respectively. The couplings are defined as

$$\begin{aligned} n^R_{im} &= \sqrt{2}g_1 N_{i1}X_{m2} + y_\mu N_{i3}X_{m1},\\ n^L_{im} &= \frac{1}{\sqrt{2}}(g_2N_{i2}+g_1N_{i1})X^*_{m1} - y_\mu N_{i3}X^*_{m2},\\ c^R_k &= y_\mu U_{k2},\\ c^L_k &= -g_2V_{k1}, \end{aligned} \quad (3)$$

where N represents neutralino, U and V are chargino mixing matrices, respectively, while X denotes the slepton mixing matrix. The muon yukawa coupling $y_\mu = g_2 m_\mu/\sqrt{2}m_W\cos\beta$ and the kinematic loop functions are defined in terms of the variables $x_{im} = m^2_{\tilde{\chi}^0_i}/m^2_{\tilde{\mu}_m}$ and $x_k = m^2_{\tilde{\chi}^\pm_k}/m^2_{\tilde{\nu}_\mu}$ and are as follows:

$$\begin{aligned} F_1^N(x) &= \frac{2}{(1-x)^4}[1-6x+3x^2+2x^3-6x^2\ln x],\\ F_2^N(x) &= \frac{3}{(1-x)^3}[1-x^2+2x\ln x],\\ F_1^C(x) &= \frac{2}{(1-x)^4}[2+3x-6x^2+x^3+6x\ln x],\\ F_2^C(x) &= -\frac{3}{2(1-x)^3}[3-4x+x^2+2\ln x]. \end{aligned} \quad (4)$$

In the limit when all the mass scales are roughly of the same order, i.e., M_{SUSY}, the sum of the above expressions in Eqs. (1) and (2) reduce to a simpler form as [27,28] (see Appendix for more detail)

$$[a_\mu^{\mathrm{SUSY}}]_{\mathrm{RPC}} \simeq 14\tan\beta\left(\frac{100\ \mathrm{GeV}}{M_{\mathrm{SUSY}}}\right)^2 10^{-10}. \quad (5)$$

Furthermore, as we have already discussed, in the absence of R-parity, the superpotential contains additional terms which are lepton and baryon number violating. In the context of our analysis we will consider only the following terms in the superpotential[1]:

$$W_{\not{R}_p} = W_{\mathrm{MSSM}} + \frac{1}{2}\lambda_{ijk}\hat{L}_i\hat{L}_j\hat{E}^c_k, \quad (6)$$

where W_{MSSM} contains the usual MSSM superfields and $\hat{L}$, $\hat{E}^c$ are the left-chiral lepton and left-chiral antilepton superfields, respectively. Gauge invariance enforces λ_{ijk} to be antisymmetric with respect to their first two indices. As a

[1]The bounds on λ' operators are more stringent compared to the bounds on λ from neutrino masses. In addition, the presence of λ' operators will increase the direct production cross section of the sneutrinos subjecting to stronger constraints on the sneutrino masses. Furthermore, we also assume the baryon number is conserved. As a result, we confine ourselves to the λ-type couplings only.

result, $\lambda_{ijk} = -\lambda_{jik}$. These RPV terms in the superpotential yield the following terms in the Lagrangian in the form as

$$\mathcal{L} = -\frac{1}{2}\lambda_{ijk}[\tilde{\nu}_{iL}\bar{l}_{kR}l_{jL} + \tilde{l}_{jL}\bar{l}_{kR}\nu_{iL} + \tilde{l}^*_{kR}\bar{\nu}^c_{iR}l_{jL} - (i \leftrightarrow j)] + \text{H.c.} \tag{7}$$

In the four component notation, the terms in Eq. (7) that contribute to $(g-2)_\mu$ can be explicitly written as

$$\mathcal{L} \subset -\lambda_{ij2}[\tilde{\nu}_{iL}\bar{\mu}P_L l_j + \tilde{l}_{jL}\bar{\mu}P_L\nu_i] - \lambda_{i2k}[\tilde{\nu}_{iL}\bar{l}_K P_L\mu + \tilde{l}^*_{kR}\bar{\nu}^c_i P_L\mu] + \text{H.c.} \tag{8}$$

In our scenario, we assume the first two generations of right chiral sleptons to be heavy to evade constraints appearing from neutrino masses and low energy observables in the presence of order one λ's as elaborated later. However, the left chiral charged sleptons/sneutrinos can be light and still avoid bounds from direct collider constraints. Therefore, in addition to the Δa_μ contribution coming from RPV operators, we also have a sizable contribution from the RPC section. The relevant diagrams contributing to $(g-2)_\mu$ are shown in Fig. 1. The generic expression of $(g-2)_\mu$ in the context of RPV MSSM is written as [16]

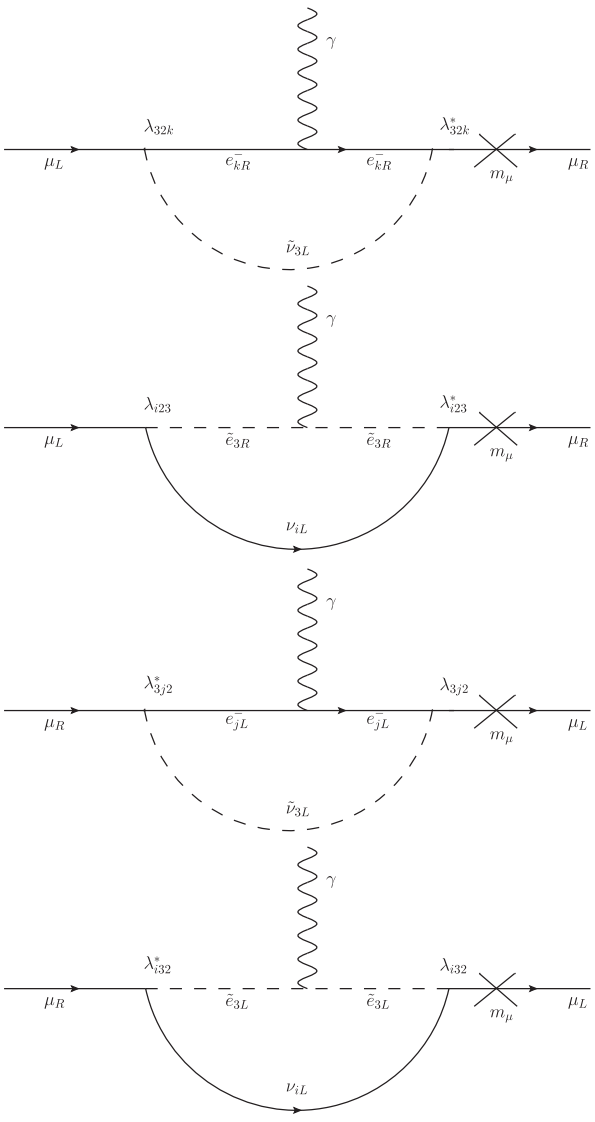

FIG. 1. The most dominant diagrams that contribute to $(g-2)_\mu$ in the RPV MSSM scenario.

$$[a^\lambda_\mu]_{\text{RPV}} = \frac{m^2_\mu}{96\pi^2}\left[|\lambda_{23k}|^2\frac{2}{m^2_{\tilde{\nu}_\tau}} + |\lambda_{3k2}|^2\left\{\frac{2}{m^2_{\tilde{\nu}_\tau}} - \frac{1}{m^2_{\tilde{\tau}_L}}\right\} - |\lambda_{k23}|^2\frac{1}{m^2_{\tilde{\tau}_R}}\right], \tag{9}$$

where $m_{\tilde{\tau}_L}$ and $m_{\tilde{\tau}_R}$ are the left and right chiral stau masses, respectively, while $m_{\tilde{\nu}_\tau}$ is the tau-sneutrino mass. In the limit where all the relevant third generation slepton masses are considered to be equal, i.e., $m_{\tilde{\tau}_L} = m_{\tilde{\tau}_R} = m_{\tilde{\nu}_\tau} = \tilde{m}$, then Eq. (9) reduces to the following simplified form:

$$[a^\lambda_\mu]_{\text{RPV}} = \frac{m^2_\mu}{32\pi^2\tilde{m}^2}\left[\frac{1}{3}|\lambda_{312}|^2 + \frac{2}{3}|\lambda_{321}|^2 + \frac{1}{3}|\lambda_{323}|^2 + |\lambda_{322}|^2 - \frac{1}{3}|\lambda_{123}|^2\right]. \tag{10}$$

An important observation is, except for λ_{322}, all the other RPV couplings come with a factor less than one. Our goal is now to study the present bounds on these couplings and to make sure if such an order one λ can be considered. We note in passing that in the present work we have taken into account all the contributions to the anomalous magnetic moment of the muon coming from both the RPC and the RPV MSSM.

III. BOUNDS ON RPV COUPLINGS

In the paradigm of SM, the lepton flavor violating (LFV) processes occur at a negligible rate due to the smallness of the neutrino masses. As a result, they are a sensitive probe of new physics and can be used to place bounds on $\not{R}_p$ couplings.[2] In order to disentangle the effects of $\not{R}_p$ interactions from the effects emerging from the possible flavor nonuniversalities in the scalar lepton sector, we assume that the slepton mass matrices are diagonal with the first two generations having equal masses. The possible sources of LFV are noted down in the following processes:

(i) Lepton flavor violating radiative decays of charged leptons: The $\not{R}_p$ interactions can in principle

[2]For bounds on trilinear R-parity violating couplings see Refs. [29–44].

generate LFV decays of charged leptons, such as $l_i \to l_j\gamma$ through one loop diagrams [45].

(ii) Lepton flavor violating decays of μ and τ into three charged leptons: The LFV decays like $l_m^- \to l_i^- l_j^- l_k^+$, where $l_m = \mu$, τ can be mediated at the tree level through t- and u-channel sneutrino exchanges when the involved leptons possess nonzero λ type $\not{R}_p$ couplings. The nonobservation of these processes results in bounds on $\lambda_{nmi}\lambda^*_{njk}$, where the sneutrino carries the index n [46].

(iii) Muon to electron conversion in nuclei: $\mu^- \to e^-$ conversion in a nucleus is normally induced by $\lambda\lambda'$ or $\lambda'\lambda'$ couplings.[3] However, $\mu^- \to e^-$ conversion in a nucleus can also proceed through photon penguin diagrams. The associated bounds can be much stronger than the ones extracted from the previously mentioned processes. The nonobservation of these processes can be translated into bounds on $\lambda\lambda$ couplings [48–50].

(iv) Charged current universality and bounds from $R_\tau/R_{\tau\mu}$: One should also take into account bounds from charged current universality that results in single bounds on the λ couplings. Similar bounds can also be obtained from the ratios $R_\tau = \Gamma(\tau \to e\nu\bar{\nu})/\Gamma(\tau \to \mu\nu\bar{\nu})$ and $R_{\tau\mu} = \Gamma(\tau \to \mu\nu\bar{\nu})/\Gamma(\mu \to e\nu\bar{\nu})$ [45].

We now tabulate the bounds on the relevant $\not{R}_p$ couplings from the nonobservation of the processes as mentioned earlier. All these limits are obtained from BP1 of Ref. [29], where the first two generations are considered to be heavy with masses around 1 TeV and the third generation is light. Making the first two generation masses heavier would further relax the bounds on $\not{R}_p$ couplings. However, we take a more conservative approach here and use the strongest limits. In addition, from the charge current universality one finds $|\lambda_{123}| \sim 0.049 \times m_{\tilde{\tau}_R}/100$ GeV. Since, in our framework, the third generation is considered to be light, hence the bounds on the particular $\not{R}_p$ operators turn out to be stringent and should be respected. From R_τ and $R_{\tau\mu}$ one finds $|\lambda_{322}| < 0.07 \times m_{\tilde{\mu}_R}/100$ GeV. Hence, in our scenario this bound can readily be relaxed by assuming a large mass for the second generation sleptons which we have considered. As mentioned earlier, this bound also translates to a lower bound on $\tilde{e}_R$ as they are considered to be degenerate with $\tilde{\mu}_R$.

From the above discussion and Table I, it is conspicuous that only one of the $\not{R}_p$ violating operators can be large [$\mathcal{O}(1)$] satisfying the above mentioned constraints. We choose it to be λ_{322}.

(i) Bound on $\not{R}_p$ couplings from neutrino mass: Neutrino masses provide serious constraints on trilinear $\not{R}_p$ couplings. In this section we will compute the impact of neutrino masses on λ_{322}. These couplings generate neutrino masses radiatively (see Fig. 2), and the generic expression is noted as [51,52]

TABLE I. Bounds on R_p couplings from low energy experiments [45,46,48–50] with specific benchmark points as shown in Ref. [29].

$\not{R}_p$ couplings	$l_i \to l_j\gamma$	$l_i \to 3l_j$	$\tau \to l_iP/\mu - e$	$l_i \to l_jl_kl_k$
$\lvert\lambda^*_{312}\lambda_{322}\rvert$	2.3×10^{-3}	8.2×10^{-4}	1.6×10^{-4}	⋯
$\lvert\lambda^*_{321}\lambda_{322}\rvert$	3.8×10^{-4}	4.1×10^{-4}	1.2×10^{-4}	⋯
$\lvert\lambda^*_{323}\lambda_{322}\rvert$	⋯	⋯	⋯	2.4×10^{-3}

$$(m_\nu)_{qm} \simeq \frac{1}{32\pi^2}\sum_{l,p}\lambda_{qlp}\lambda_{mpl}m_l \sin 2\phi_l \ln\left(\frac{M^2_{p1}}{M^2_{p2}}\right), \tag{11}$$

where m_l is the mass of the lepton, ϕ_l is the mixing angle obtained by diagonalizing the charged slepton mass squared matrix, which takes the form

$$\sin 2\phi_l = \frac{2Am_l}{\sqrt{(L^2-R^2)^2 + 4A^2m_l^2}}, \tag{12}$$

where $L^2 \equiv (m^2_{\tilde{L}})_{ll} + (T_3 - e\sin^2\theta_W)m_Z^2\cos 2\beta$, $R^2 \equiv (m^2_{\tilde{E}})_{ll} + (e\sin^2\theta_W)m_Z^2\cos 2\beta$, with $T_3 = -1/2$ and $e = -1$ for the down-type charged sleptons, and the effective trilinear scalar coupling term is denoted as $A \equiv (A_E)_{0ll} - \mu\tan\beta$. M_{p1} and M_{p2} are slepton mass eigenstates obtained by diagonalizing the slepton mass squared matrix. The trilinear $\not{R}_p$ operator under consideration, i.e., λ_{322} gives mass to the (33) element of the neutrino mass matrix. As a result, Eq. (11) can be simplified to

$$(m_\nu)_{33} \simeq \frac{1}{16\pi^2}|\lambda_{322}|^2\frac{Am_\mu^2}{\sqrt{(L^2-R^2)^2 + 4A^2m_l^2}} \times \ln\left(\frac{M^2_{p1}}{M^2_{p2}}\right). \tag{13}$$

Considering the central values for the neutrino mass squared and mixing parameters [53] (with the choice

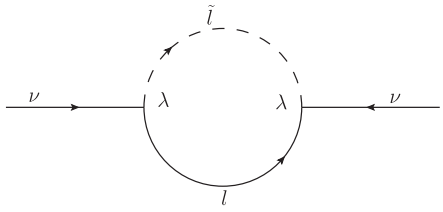

FIG. 2. Trilinear R_p violating contribution to neutrino masses.

[3]For a theoretical calculation of this process in R-parity violating SUSY models, we refer the reader to Ref. [47].

of CP violating phase $\delta = 0$), the central value of element 33 of the neutrino mass matrix for normal and inverted hierarchy becomes

$$(m_\nu)^{NH}_{33} = 0.023 \text{ eV},$$
$$(m_\nu)^{IH}_{33} = 0.031 \text{ eV}. \quad (14)$$

From Eq. (13), it is straightforward to show that in the limit $(R^2 \gg L^2) \equiv \tilde{m}^2 \gg A^2$, the same equation gives the following bound on the A parameter as

$$A \ln\left(\frac{M_{p1}}{M_{p2}}\right) \leq \mathcal{O}(10) \text{ GeV}, \quad (15)$$

for $\mathcal{O}(1)$ λ_{322} and $\tilde{m}$; i.e., the first two generations of the right slepton masses are in the ballpark of $\mathcal{O}(10 \text{ TeV})$. Therefore, we observe that in order to consider $\lambda_{322} \sim \mathcal{O}(1)$, one needs to satisfy Eq. (15),[4] which invokes a cancellation between the soft SUSY breaking A term in the charged slepton sector and the μ term.

IV. NUMERICAL ANALYSIS AND BENCHMARKS

From the previous discussions, it is clear that only λ_{322} plays a dominating role in ameliorating the tension between the observed muon anomalous magnetic moment and the SM expectation. In the limit when only λ_{322} is nonzero, whereas all the other trilinear $\not{R}_p$ violating couplings are vanishingly small, Eq. (10) further simplifies to [16]

$$[a^\lambda_\mu]_{\text{RPV}} \simeq 34.9 \times 10^{-10} \left(\frac{100 \text{ GeV}}{\tilde{m}}\right)^2 |\lambda_{322}|^2. \quad (16)$$

It is conspicuous that an order one coupling can explain the muon anomalous magnetic moment event within 1σ of the central measured value.

In order to have a complete and concrete picture, we use the trilinear R-parity violating model implemented in SARAH v-4.4.6 [56,57]. The spectrum has been generated using SPheno v-3.3.3 [58,59]. FlavorKit [60] is used to ensure that the benchmark points are consistent with all relevant flavor violating observations. We fix the following parameters, such as the bino mass parameter $M_1 = 300$ GeV, the wino mass parameter $M_2 = 1.7$ TeV, the Higgsino mass term $\mu = 200$ GeV, the gluino mass $M_3 = 1.5$ TeV, $\tan\beta = v_u/v_d = 20$, and the mass of the CP-odd Higgs $M_A = 400$ GeV. λ_{322} is varied from 0.5 to 1.2 keeping all other $\not{R}_p$ couplings to zero.[5] We also vary the soft mass squared term of the slepton doublet in the limit $3 \times 10^4 \text{ GeV}^2 \leq (m^L_{33})^2 \leq 2.5 \times 10^5 \text{ GeV}^2$ and chalk out the parameter space by putting the Δa_μ constraints within 1σ and 2σ regimes.

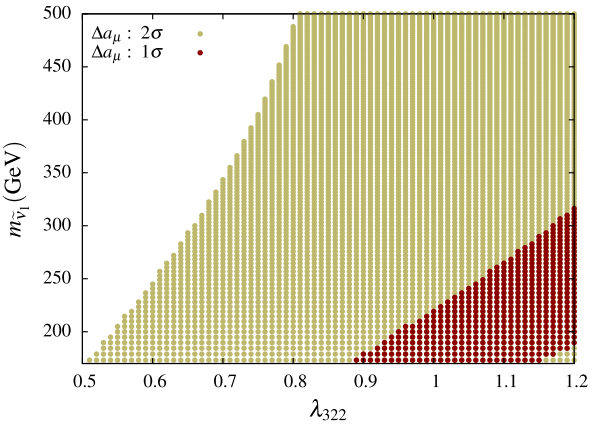

FIG. 3. 1 and 2σ limits on Δa_μ are shown in red and yellow colours respectively in the $m_{\tilde{\nu}_1} - \lambda_{322}$ plane where $m_{\tilde{\nu}_1} \equiv m_{\tilde{\nu}_\tau}$.

In Fig. 3 we show the 1σ and 2σ constraints on Δa_μ in the $m_{\tilde{\nu}_1} - \lambda_{322}$ plane where $\tilde{\nu}_1$ is the lightest mass eigenstate of the sneutrinos with $\tilde{\nu}_1 \equiv \tilde{\nu}_\tau$. We observe that the 1σ regime of this parameter can be reached for large values of $\lambda_{322} \geq 0.9$ and in the low mass limit of m^L_{33}, which also controls the left sneutrino and left charged slepton masses. From Eq. (8), a nonzero λ_{322} implies the tau-sneutrino decays to a $\mu^+\mu^-$ final state. It is important to note that pair produced tau-sneutrinos decaying via the 4μ final state has not been looked at by both the ATLAS and CMS collaborations. However, experiments have looked for pair production of $\tilde{\mu}_L$, which decays to the μ and χ^0_1, and placed a mass limit on $\tilde{\mu}$. Now, in our case, the stau $\tilde{\tau}_L$ associated with $\tilde{\nu}_\tau$ can decay to $\mu\nu_\mu$, and thus a pair produced stau would give same final state topology through the same RPV operator. Hence, the present bound on $\tilde{\mu}$ can be attributed to $\tilde{\tau}$ (and hence $\tilde{\nu}_\tau$) in our case. The present lower bound on $\tilde{\mu}$ stands at 300 GeV [12,13], and thus this bound can also be mapped to an lower bound on the $\tilde{\nu}_\tau$ mass. However, it is also important to note that by reducing the branching ratio of $\tilde{\nu}_\tau \to \mu^+\mu^-$, one can relax the bound considerably. For example, we check that for $\text{BR}(\tilde{\nu}_\tau \to \mu^+\mu^-) \sim 70\%$, the bound on the sneutrino mass reduces to 250 GeV, while for $\text{BR}(\tilde{\nu}_\tau \to \mu^+\mu^-) \sim 50\%$ the bound on the same is around 220 GeV.

In our scenario, the partial decay width of the sneutrino (in this case the tau sneutrino) decaying to $\ell^+\ell^-$ is given by

$$\Gamma(\tilde{\nu}_i \to l^+_j l^-_k) \simeq \frac{1}{16\pi} \lambda^2_{ijk} m_{\tilde{\nu}_i}. \quad (17)$$

Further, if kinematically allowed, the sneutrino can also undergo a two body decay with a tau neutrino and a neutralino or a tau lepton associated with a chargino in the

[4]The issues pertaining to neutrino masses and muon $(g-2)$ anomaly in the framework of RPV SUSY can also be found in Refs. [54,55].

[5]In order satisfy the muon $(g-2)$ and the LEP bound on the sneutrino mass simultaneously leads to $\lambda_{322} \geq 0.5$, however we restrict ourselves within $\lambda_{322} \leq 1.2$.

final state. The neutralino and chargino would also undergo a three body decay in the RPV framework. The two body decay widths of the sneutrino are noted below [61],

$$\Gamma(\tilde{\nu} \to \tilde{\chi}_j^0 \nu) = \frac{g^2 |Z_{iZ}|^2 m_{\tilde{\nu}}}{32\pi \cos^2\theta_W} B(m^2_{\tilde{\chi}_j^0}/m^2_{\tilde{\nu}}),$$
$$\Gamma(\tilde{\nu} \to \tilde{\chi}^+ \ell^-) = \frac{g^2 |V_{11}|^2 m_{\tilde{\nu}}}{16\pi} B(m^2_{\tilde{\chi}^+}/m^2_{\tilde{\nu}}), \qquad (18)$$

where V_{11} is one of the mixing matrix elements in the chargino sector and Z_{jZ} is the neutralino mixing matrix element. The B function is defined as $B(x) = (1-x)^2$. In the presence of large λ_{322}, which is also motivated from the perspective of fitting Δa_μ, the partial decay width of the sneutrino decaying to a pair of leptons will dominate over the other decay modes. In Fig. 4, we portray the branching ratios of the lightest sneutrino as a function of its mass. During this scan, we ensure that all the points satisfy the Higgs mass and branching ratio constraints and also the low energy experimental constraints. In addition, care has been taken in removing all the tachyonic states from the scan. The points are also consistent within the 2σ error of the Δa_μ parameter.

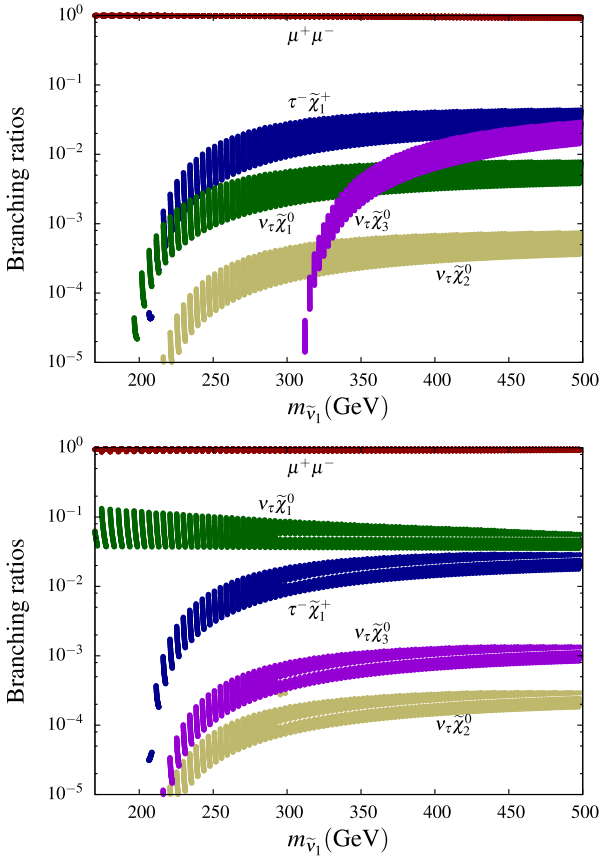

FIG. 4. Decay branching ratios of the lightest sneutrino for bino-line neutralino mass parameters of $M_1 = 300$ GeV and $M_1 = 10$ GeV, respectively. The points are consistent within the 2σ error of the Δa_μ parameter.

parameter. All the parameters are fixed at the previously mentioned values except for M_1. In the first column of Fig. 4, M_1 is fixed at 300 GeV, while in the lower panel $M_1 = 10$ GeV. As a result, the sneutrino decays to charginos with associated leptons, and neutrino + neutralino final states are highly suppressed due to phase space consideration. However, the binolike neutralino mass parameter can be light (we choose it to be 10 GeV). There are two major constraints for the light binolike neutralino; for example, one has to check if the Higgs partial decay width into this channel is satisfied or not, and second, in the RPV scenario, the light neutralino can decay into final states involving fermions and can avoid constraints from its overproduction in the early universe [62,63]. In addition, the added advantage of this scenario is the presence of the light neutralino opens up new decay modes of the sneutrino. Thus the effective branching ratio of this sneutrino decaying to the two muon final state can be reduced. As a result, the branching ratio of the stau decaying to $\mu\nu_\mu$ also reduces and thus relaxes the bound on the left handed stau mass. This in turn also implies the left-chiral sneutrino mass bounds can be relaxed further as both the masses are controlled by the same parameter. Before we proceed any further, let us give a brief outline of the search for heavy di-muon resonances at the Tevatron and LHC experiments.

Heavy resonances decaying to a pair of muons naturally comes in many extensions of the SM with additional gauge groups. Both the ATLAS and CMS collaborations have searched for the heavy spin-1 resonance Z' via di-muon final states at the 7 and 8 TeV runs of LHC [64–66]. Nonobservation of signatures of the signal events leads to the 95% C.L. upper limits on the production cross section times branching ratios over a range of di-muon invariant masses. In Fig. 5, the black dotted and red dashed lines indicate the corresponding limits obtained from the ATLAS and CMS collaborations by the LHC-8 data, respectively. Moreover, the CDF collaboration at the Tevatron experiment has also performed a study of di-muon resonances from the direct production of a sneutrino or Z' with

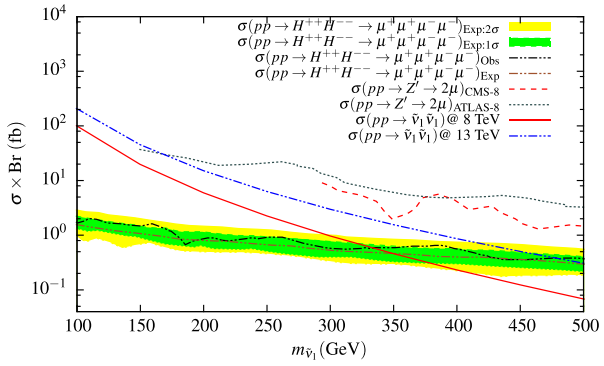

FIG. 5. Present 95% C.L. upper limits on the $\sigma \times BR$ for different values of heavy resonance masses.

1.96 TeV data [67,68]. However, we do not consider the bounds coming from the sneutrino production since it involves the λ' type coupling in the production process which we set to be zero throughout our analysis. We find that our di-muon resonances, shown in blue dashed double-dotted (13 TeV) and red solid (8 TeV) lines, have smaller cross sections compared to the ATLAS and CMS limits as elaborated later in the text.

Furthermore, we also consider the present bounds obtained from exotic searches at the LHC with final state topologies similar to ours, i.e., with four muons among which two are positively charged and two are negatively charged [69]. The ATLAS collaboration has searched for doubly charged Higgs bosons decaying to a pair of same sign muons, thus giving rising to the same final state signature. We again translate the 95% C.L. upper limit on the production cross-section times branching ratio for heavy resonance mass from 100 to 500 GeV. The black dashed double-dotted line indicates the 95% C.L. upper limit on the cross-section times branching ratio, while the green and yellow regions denote the 1σ and 2σ bands around the expected line shown with the brown dashed double-dotted line. From Fig. 5, we see that if one allows 2σ fluctuations, then a sneutrino mass less than 290 GeV is excluded from this exotic search.

It is to be noted that, since we set λ' to zero, the sneutrinos are produced at the LHC via only Higgs boson and off-shell Z mediation, and the cross section naturally becomes much smaller compared to the present upper bounds except for the doubly charged Higgs boson search process. The bound on the di-muon mass and hence on the sneutrino mass stands roughly at 290 GeV, similar to what we obtain translating the LHC bounds on the sleptons from the direct searches. Keeping all these bounds in mind, in Table II we show the benchmark points pertaining to two relevant scenarios under consideration. The parameters that are fixed are $\tan\beta = 20$, $\mu = 200$ GeV, $M_A = 400$ GeV, $M_2 = 1.7$ TeV, $M_3 = 1.5$ TeV, $A_t = -1.9$ TeV, $\lambda_{322} = 1.2$, $(m_L^2)_{33} = 8.92 \times 10^4 (\text{GeV})^2$, and $1.1 \times 10^5 (\text{GeV})^2$, respectively. M_1 is fixed at 10 GeV (BP1) and 300 GeV (BP2), respectively. The obtained Δa_μ is within the 2σ error bar of the central value.

TABLE II. Mass spectrum and a few observables for the two benchmark points.

Point	BP1	BP2
Mass spectrum		
h (GeV)	124.2	124.3
H^0 (GeV)	413	410
$H^\pm$ (GeV)	421	418
$\tilde{g}$ (GeV)	1622	1622
$\tilde{t}_1$ (GeV)	835	835
$\tilde{\nu}_1$ (GeV)	291	323
$\tilde{\chi}_1^\pm$ (GeV)	204	204
$\tilde{\chi}_2^\pm$ (GeV)	1711	1711
$\tilde{\chi}_1^0$ (GeV)	9	310
$\tilde{\chi}_2^0$ (GeV)	206	208
$\tilde{\chi}_3^0$ (GeV)	210	309
$\tilde{\chi}_4^0$ (GeV)	1711	1711
$BR(b \to s\gamma) \times 10^4$	2.57	2.57
$BR(B_s \to \mu^+\mu^-) \times 10^9$	3.96	3.98
$\Delta a_\mu \times 10^{10}$	19.6	19.7

V. COLLIDER ANALYSIS

The search for the new physics signatures with multiple leptons has always been considered as the golden channel mostly due to the cleanliness of the final state topology. Both the ATLAS and CMS collaborations at the LHC have searched for new resonances via lepton-rich signatures in the context of R-parity violating MSSM [70–72]. However, the final state topologies that have been studied by the CDF collaborations at the Tevatron and ATLAS collaborations at the LHC include heavy neutral particles decaying to $e\mu$, $e\tau$, or $\mu\tau$ [70,73]. From their analysis, we find that the $e\mu$ channel provides the best sensitivity due to better resolution for the electrons and muons (see Fig. 2 of Ref. [70]). In this paper, we study possibly the cleanest final state topology that contains four isolated muons, which comes from the pair production of the lightest sneutrino ($\tilde{\nu}_1 \equiv \tilde{\nu}_\tau$) which subsequently decays to a pair of muons through a nonzero λ_{322} R-parity violating coupling. We reiterate that this channel is also interesting from the perspective of the $(g-2)_\mu$ anomaly.

We perform the collider analysis for the two benchmark points already introduced. We generate signal events using MadGraph (v5 2.2.2) [74] where the main sneutrino pair production channel involves Z mediation. We then pass the events to PYTHIA (v 6.4.28) [75] for hadronization and showering with the CTEQ6L1 [76] parton density function. The final state of interest contains four isolated muons with no real source of missing energy. The possible SM backgrounds that can mimic the signal topology are as follows: (i) SM Higgs boson production via gluon-gluon fusion, vector boson fusion, associated production processes with the $H \to ZZ^* \to 4\mu$ final state. (ii) Direct production of a pair of SM gauge bosons, i.e., WW, WZ, and ZZ with W/Z decay leptonically. (iii) Z + jets and $t\bar{t}$ processes.[6] Similar to the signal events, the background processes are also simulated using MadGraph and then passed to PYTHIA. After generating the signal and background events, we apply the following kinematic cuts, which are more or less in line with those applied in a similar analysis by ATLAS collaboration [70]. We select the events with four isolated muons with $p_T > 10$ GeV and $|\eta| < 2.5$. The isolation criteria imposed on the muons are (a) that the angular

[6]We check that processes like $t\bar{t}Z$, $t\bar{t}H$ with $H \to ZZ^*$ triple gauge boson productions contribute to a negligible amount. So, we display only the dominant backgrounds in the table.

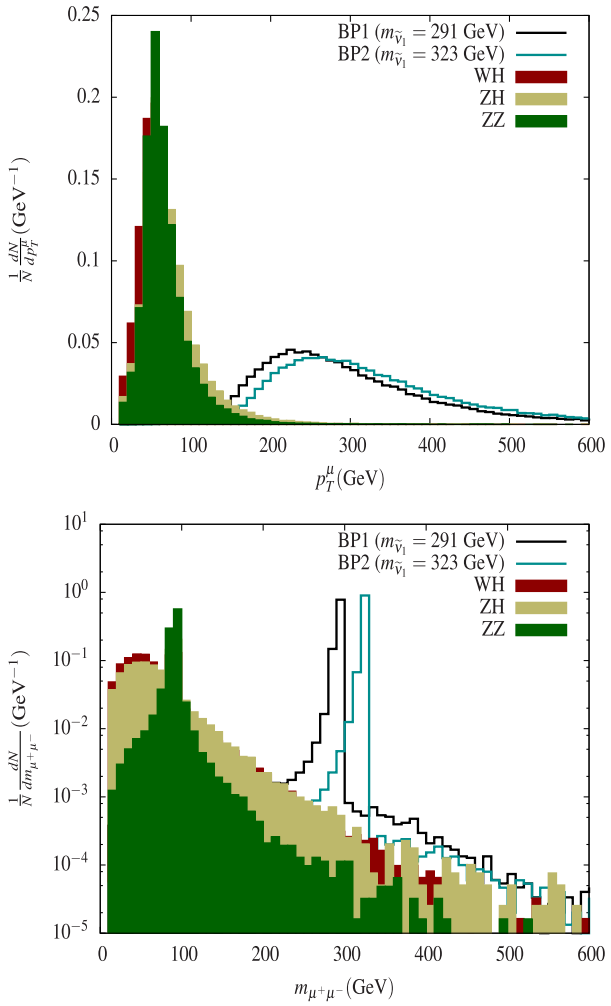

FIG. 6. Upper: The p_T distribution of the leading muon for the two benchmark points BP1 and BP2 along with the three dominant SM backgrounds. The signal muons are seen to be harder compared to that of the SM ones. Lower: Di-muon invariant mass distribution for the signal and background events. Sharp resonance peaks can be observed for the signal benchmark points, while a clear peak at $M_Z \sim 91$ GeV is also visible for the mass distribution.

separation $\Delta R_{\ell J}$ between the lepton and jets[7] should not be less than 0.4, and (b) that the sum of the scalar p_T of all stable visible particles within a cone of radius $\Delta R = 0.2$ around the lepton should not exceed 10 GeV. In Fig. 6, we display the p_T distribution of the leading isolated muon. Note that, for the signal events the leptons are relatively harder compared to SM backgrounds, and this important feature can be used as a trigger of such events. For our signal events, the muons are coming from the "on-shell" decay of the sneutrino ($\tilde{\nu}_1$), and thus one can reconstruct the $\tilde{\nu}_1$ mass using the di-leptonic invariant mass. However, for processes like ZH, WH with $H \to ZZ^*$, one Z is on-shell

[7]We reconstruct jets using FASTJET v3.1.0 [77] with an anti-k_T jet algorithm and jet radius $R = 0.4$.

TABLE III. Event summary for the signal and background events. The quantities σ_0 and $\sigma_{\rm eff}$ represent the production cross section and the effective cross section, respectively. The total cross section is denoted by $\sigma_{\rm tot}$. For the WH and ZH processes the Higgs boson is assumed to decay to ZZ^* with Z decaying to two muons. We calculate the signal significance $\mathcal{S} = S/\sqrt{(S+B)}$ with $\mathcal{L} = 100$ fb^{-1} where S and B are the total number of signal and background events.

Process	σ_0 (fb)	$\sigma_{\rm eff}$ (fb)	$\sigma_{\rm tot}$ (fb)	Significance
$\tilde{\nu}_1\tilde{\nu}_1^*$	4.08 (BP1)	1.512	1.512	
	2.64 (BP2)	0.98	0.98	
WH	1380 [79]	0.014		8.4 (BP1)
ZH	868 [79]	0.0022	1.716	5.9 (BP2)
ZZ	15000 [80]	1.7		

while the other is off-shell, and thus the di-muon invariant mass will have a long tail with a sharp peak at $M_Z \sim 91$ GeV. Among all possible di-muon invariant mass recombinations, the one with minimum mass difference $\Delta m = |m_{12} - m_{34}|$ is selected where m_{12} and m_{34} are two such di-muon invariant masses. We impose a Z veto by requiring either of the di-muon invariant masses to be greater than 100 GeV. Note that by making such a choice we also reduce the contributions coming from processes like the associated production of a Z boson with J/ψ and/or Υ significantly. In the lower panel of Fig. 6, the dimuon invariant masses are shown for both the signal and the background events, where for the signal events we show for two representative benchmark points BP1 and BP2 with masses ~290 GeV and 320 GeV, respectively. From the figure it is evident that a cut on the di-muon invariant mass $m_{\mu\mu} > 100$ GeV would help us to reduce the dominant SM backgrounds.

In Table III, we show the production cross section (σ_0), the effective cross section ($\sigma_{\rm eff} = \sigma_0 \times \epsilon$, with ϵ being the cut efficiency) for the two benchmark points BP1 and BP2 along with the three dominant SM backgrounds WH, ZH, and ZZ with $H \to ZZ^*$. The cross sections for the signal events are calculated using MadGraph at the leading order,[8] while we follow the LHC Higgs Cross Section Working Group report [79] for the WH, ZH backgrounds where they are calculated at next-to-next-to leading order QCD and next-to leading order (NLO) EW. The cross section for ZZ has been taken from Ref. [80], calculated at NLO QCD and NLO EW. The statistical significance ($\mathcal{S}$) is calculated as $\mathcal{S} = S/\sqrt{(S+B)}$, where S and B are the total number of signal and background events, respectively, for $\mathcal{L} = 100$ fb^{-1} luminosity at the 13 TeV run of LHC. From Table III one can infer that the lightest sneutrinos with masses around 300–320 GeV can be discovered using this

[8]We use Prospino [78] to calculate the K-factor associated with the slepton pair production process and find $K = 1.2$ for slepton masses from 200 to 500 GeV.

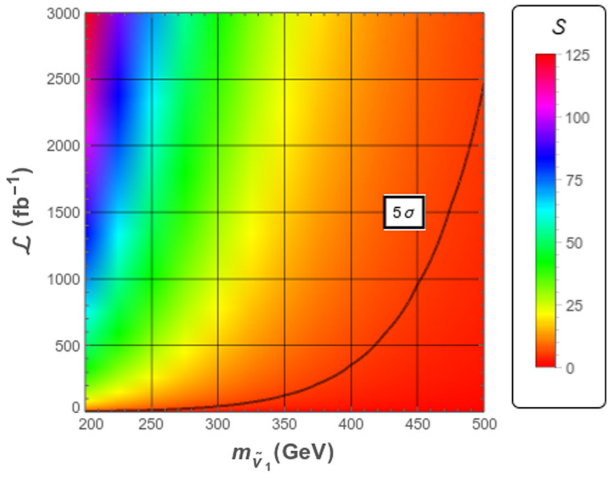

FIG. 7. Contour plot in the $\mathcal{L} - m_{\tilde{\nu}_1}$ plane for the binolike neutralino mass parameter of $M_1 = 300$ GeV. A similar distribution can be obtained for $M_1 = 10$ GeV.

4μ golden channel at the early run of 13 TeV LHC. In order to estimate the reach of the sneutrinos at the 13 TeV LHC, we now vary the soft-mass parameter $(m_L^2)_{33}$ in such a way that the sneutrino mass varies from 200 GeV to 500 GeV keeping all other parameters the same as BP1 and BP2. For each point we again calculate the statistical significance $\mathcal{S}$ as already defined and then vary the luminosity $\mathcal{L}$. In Fig. 7, we display the statistical signal $\mathcal{S}$ in the $\mathcal{L} - m_{\tilde{\nu}_1}$ plane. The black solid line indicates the required luminosity for a given sneutrino mass in order to obtain a 5σ statistical significance. We find that by using the four muon golden channel one can probe the sneutrino masses up to 450 GeV with 1000 fb^{-1} of luminosity at the 13 TeV LHC.

VI. CONCLUSIONS

We revisit the possibility of satisfying the anomalous magnetic moment of the muon in the paradigm of R-parity violating MSSM. The relevant coupling, λ_{322}, which plays a major role in this process is identified. The low energy and neutrino mass constraints have been checked and can be rather easily satisfied even at the presence of an $\mathcal{O}(1)$ value of this particular R-parity violating coupling. We show that this explanation of having large muon $(g-2)$ via R-parity violation can be tested directly at the LHC. An artifact of $\mathcal{O}(1)$ λ_{322} is the decay of the pair produced tau sneutrino into a final state comprising four muons. This is a so-called "golden channel" because of large signal efficiency and a minuscule contribution from the SM backgrounds. We analyze all the relevant SM backgrounds and find that sneutrino masses up to 450 GeV can be probed with an integrated luminosity of 1000 fb^{-1} at the 13 TeV LHC. Such a channel is yet to be investigated by both the ATLAS and CMS collaborations, and it is our hope that this work will motivate them to perform a dedicated analysis in this direction in the near future.

ACKNOWLEDGMENTS

A. C. and S. C. would like to thank the Department of Atomic Energy, Government of India, for financial support. We gratefully acknowledge Sreerup Raychaudhuri, Gautam Bhattacharyya, Sourov Roy, Tuhin S. Roy, and Biplob Bhattacherjee for useful discussions. S. C. also thanks Florian Staub for helpful discussions regarding SARAH.

APPENDIX: MUON $g-2$ IN RPC MSSM

In this appendix we elaborate the SUSY-RPC contribution to the anomalous magnetic moment of the muon [14,27,28]. In general the chargino-sneutrino loop dominates over the neutralino-smuon loop. We reiterate that when all the mass scales are of the same order, the chargino-sneutrino loop contribution shown in Eq. (2) reduces to the form

$$\begin{aligned}\delta a_\mu^{\tilde{\chi}^\pm} &= \frac{m_\mu}{16\pi^2}\left\{\frac{m_\mu}{12M_S^2}\left(\frac{m_\mu^2}{2M_S^2\cos^2\beta}\overset{0}{\nearrow}+g_2^2\right)+\frac{2g_2}{3M_S}\frac{m_\mu g_2}{\sqrt{2}M_S\cos\beta}\right\}\\ &= \frac{m_\mu^2}{192\pi^2M_s^2}\left\{g_2^2+\frac{4\sqrt{2}g_2^2}{\cos\beta}\right\}\\ &\simeq \frac{m_\mu^2 g_2^2}{192\pi^2M_s^2}\left\{1+\frac{6}{\cos\beta}\right\}.\end{aligned} \tag{A1}$$

In the large $\tan\beta$ limit, Eq. (A1) can be further simplified to

$$\begin{aligned}\delta a_\mu^{\tilde{\chi}^\pm} &\simeq \frac{m_\mu^2 g_2^2}{192\pi^2M_s^2}\times\frac{6}{\cos\beta}\\ &\simeq \frac{m_\mu^2 g_2^2}{32\pi^2M_s^2}\tan\beta.\end{aligned} \tag{A2}$$

Similarly, the neutralino-smuon contribution can be written down under the same approximation as

$$\delta a_\mu^{\tilde{\chi}^0} = \frac{m_\mu^2}{192\pi^2M_s^2}(g_1^2-g_2^2)\tan\beta. \tag{A3}$$

Therefore, the total RPC-SUSY contribution converges to the form given in Eq. (5). An interesting point to note is that although the one loop contributions $a_\mu^{\tilde{\chi}^{0,\pm}}$ have terms linear in $m_{\tilde{\chi}^{0,\pm}}$ [see Eqs. (1) and (2)], they are not enhanced by $m_{\tilde{\chi}^{0,\pm}}$ as compared to the other terms [14]. The reason is that these terms also involve either a factor of y_μ or $X_{m1}X_{m2}$, which is again proportional to $(M_\mu^2)_{12}$ and therefore to y_μ. Hence, all the RPC contributions to $(g-2)_\mu$ are of the order of m_μ^2/M_s^2 as shown explicitly. On the other hand, for $\mathcal{O}(1)$ RPV λ type couplings the contribution to a_μ also turns out to be of the same order as its RPC counterpart.

[1] G. Aad *et al.* (ATLAS Collaboration), Phys. Lett. B **716**, 1 (2012); S. Chatrchyan *et al.* (CMS Collaboration), Phys. Lett. B **716**, 30 (2012).

[2] G. W. Bennett *et al.* (Muon $g-2$ Collaboration), Phys. Rev. D **73**, 072003 (2006).

[3] For reviews on supersymmetry, see, e.g., H. P. Nilles, Phys. Rep. **110**, 1 (1984); J. D. Lykken, arXiv:hep-th/9612114; J. Wess and J. Bagger, *Supersymmetry and Supergravity* (Princeton University Press, Princeton, NJ, 1991), 2nd ed.

[4] H. E. Haber and G. Kane, Phys. Rep. **117**, 75 (1985); S. P. Martin, Adv. Ser. Dir. High Energy Phys. **21**, 1 (2010); D. Chung, L. Everett, G. Kane, S. King, J. Lykken, and L. Wang, Phys. Rep. **407**, 1 (2005).

[5] M. Drees, P. Roy, and R. M. Godbole, *Theory and Phenomenology of Sparticles* (World Scientific, Singapore, 2005); H. Baer and X. Tata, *Weak Scale Supersymmetry: From Superfields to Scattering Events* (Cambridge University Press, Cambridge, UK, 2006).

[6] A. Djouadi, Phys. Rep. **459**, 1 (2008).

[7] T. Aoyama, M. Hayakawa, T. Kinoshita, and M. Nio, Phys. Rev. Lett. **109**, 111808 (2012); A. Czarnecki, W. J. Marciano, and A. Vainshtein, Phys. Rev. D **67**, 073006 (2003); Phys. Rev. D **73**, 119901(E) (2006).

[8] F. Jegerlehner and A. Nyffeler, Phys. Rep. **477**, 1 (2009); K. Melnikov and A. Vainshtein, Springer Tracts Mod. Phys. **216**, 1 (2006); S. Peris, M. Perrottet, and E. de Rafael, Phys. Lett. B **355**, 523 (1995); A. Czarnecki, B. Krause, and W. J. Marciano, Phys. Rev. D **52**, R2619 (1995); C. Gnendiger, D. Stöckinger, and H. Stöckinger-Kim, Phys. Rev. D **88**, 053005 (2013).

[9] G. Aad *et al.* (ATLAS Collaboration), J. High Energy Phys. 10 (2015) 054.

[10] V. Khachatryan *et al.* (CMS Collaboration), J. High Energy Phys. 04 (2015) 124.

[11] ATLAS SUSY search results summary page, https://twiki.cern.ch/twiki/bin/view/AtlasPublic/SupersymmetryPublicResults CMS SUSY search results summary page, https://twiki.cern.ch/twiki/bin/view/CMSPublic/PhysicsResultsSUS.

[12] G. Aad *et al.* (ATLAS Collaboration), J. High Energy Phys. 05 (2014) 071.

[13] V. Khachatryan *et al.* (CMS Collaboration), Eur. Phys. J. C **74**, 3036 (2014).

[14] D. Stockinger, J. Phys. G **34**, R45 (2007).

[15] G. Bhattacharyya, Nucl. Phys. B, Proc. Suppl. **52A**, 83 (1997); , in *Beyond the Desert 1997: Tegernsee 1997* (CRC Press, Boca Raton, FL, 1998), pp. 194–201; R. Barbier *et al.*, Phys. Rep. **420**, 1 (2005); H. K. Dreiner, in *Perspectives on Supersymmetry*, edited by G. L. Kane, Advanced Series on Directions in High Energy Physics Vol. 21 (World Scientific, Singapore, 2010), pp. 565–583.

[16] J. E. Kim, B. Kyae, and H. M. Lee, Phys. Lett. B **520**, 298 (2001).

[17] U. Chattopadhyay and P. Nath, Phys. Rev. Lett. **86**, 5854 (2001).

[18] U. Chattopadhyay and P. Nath, Phys. Rev. D **53**, 1648 (1996).

[19] U. Chattopadhyay, D. K. Ghosh, and S. Roy, Phys. Rev. D **62**, 115001 (2000).

[20] D. K. Ghosh, P. Roy, and S. Roy, J. High Energy Phys. 05 (2012) 067.

[21] M. Chakraborti, U. Chattopadhyay, A. Choudhury, A. Datta, and S. Poddar, J. High Energy Phys. 07 (2014) 019.

[22] B. Bhattacherjee and A. Chakraborty, Phys. Rev. D **89**, 115016 (2014).

[23] J. Chakrabortty, A. Choudhury, and S. Mondal, J. High Energy Phys. 07 (2015) 038.

[24] G. Bhattacharyya, B. Bhattacherjee, T. T. Yanagida, and N. Yokozaki, Phys. Lett. B **730**, 231 (2014).

[25] G. Bhattacharyya, K. B. Chatterjee, and S. Nandi, Nucl. Phys. **B831**, 344 (2010).

[26] B. P. Padley, K. Sinha, and K. Wang, Phys. Rev. D **92**, 055025 (2015).

[27] S. P. Martin and J. D. Wells, Phys. Rev. D **64**, 035003 (2001).

[28] T. Moroi, Phys. Rev. D **53**, 6565 (1996); **56**, 4424(E) (1997).

[29] H. K. Dreiner, K. Nickel, F. Staub, and A. Vicente, Phys. Rev. D **86**, 015003 (2012).

[30] H. K. Dreiner, M. Kramer, and B. O'Leary, Phys. Rev. D **75**, 114016 (2007).

[31] H. K. Dreiner, M. Hanussek, and S. Grab, Phys. Rev. D **82**, 055027 (2010).

[32] J. P. Saha and A. Kundu, Phys. Rev. D **66**, 054021 (2002).

[33] J. P. Saha and A. Kundu, Phys. Rev. D **69**, 016004 (2004).

[34] A. Kundu and J. P. Saha, Phys. Rev. D **70**, 096002 (2004).

[35] A. de Gouvea, S. Lola, and K. Tobe, Phys. Rev. D **63**, 035004 (2001).

[36] M. Chaichian and K. Huitu, Phys. Lett. B **384**, 157 (1996).

[37] G. Bhattacharyya, J. R. Ellis, and K. Sridhar, Mod. Phys. Lett. A **10**, 1583 (1995).

[38] K. Agashe and M. Graesser, Phys. Rev. D **54**, 4445 (1996).

[39] D. K. Ghosh, S. Raychaudhuri, and K. Sridhar, Phys. Lett. B **396**, 177 (1997).

[40] D. K. Ghosh, X. G. He, B. H. J. McKellar, and J. Q. Shi, J. High Energy Phys. 07 (2002) 067.

[41] G. Bhattacharyya and P. B. Pal, Phys. Rev. D **59**, 097701 (1999).

[42] A. Abada and M. Losada, Phys. Lett. B **492**, 310 (2000).

[43] B. C. Allanach, A. Dedes, and H. K. Dreiner, Phys. Rev. D **69**, 115002 (2004); Phys. Rev. D **72**, 079902(E) (2005).

[44] L. S. Littenberg and R. Shrock, Phys. Lett. B **491**, 285 (2000).

[45] J. Adam *et al.* (MEG Collaboration), Phys. Rev. Lett. **107**, 171801 (2011).

[46] K. A. Olive *et al.* (Particle Data Group Collaboration), Chin. Phys. C **38**, 090001 (2014).

[47] I. H. Lee, Phys. Lett. **138B**, 121 (1984); I. H. Lee, Nucl. Phys. **B246**, 120 (1984).

[48] C. Dohmen *et al.* (SINDRUM II Collaboration), Phys. Lett. B **317**, 631 (1993).

[49] W. Honecker *et al.* (SINDRUM II Collaboration), Phys. Rev. Lett. **76**, 200 (1996).

[50] W. H. Bertl *et al.* (SINDRUM II Collaboration), Eur. Phys. J. C **47**, 337 (2006).

[51] Y. Grossman and H. E. Haber, Phys. Rev. D **59**, 093008 (1999).

[52] Y. Grossman and S. Rakshit, Phys. Rev. D **69**, 093002 (2004).

[53] D. V. Forero, M. Tortola, and J. W. F. Valle, Phys. Rev. D **90**, 093006 (2014).

[54] R. Adhikari and G. Rajasekaran, arXiv:hep-ph/0107279.
[55] R. Adhikari, E. Ma, and G. Rajasekaran, Phys. Rev. D **65**, 077703 (2002).
[56] F. Staub, arXiv:0806.0538.
[57] F. Staub, Adv. High Energy Phys. **2015**, 840780 (2015).
[58] W. Porod, Comput. Phys. Commun. **153**, 275 (2003).
[59] W. Porod and F. Staub, Comput. Phys. Commun. **183**, 2458 (2012).
[60] W. Porod, F. Staub, and A. Vicente, Eur. Phys. J. C **74**, 2992 (2014).
[61] Y. Grossman and H. E. Haber, Phys. Rev. Lett. **78**, 3438 (1997).
[62] H. K. Dreiner, S. Heinemeyer, O. Kittel, U. Langenfeld, A. M. Weber, and G. Weiglein, Eur. Phys. J. C **62**, 547 (2009).
[63] S. Chakraborty and S. Roy, J. High Energy Phys. 01 (2014) 101.
[64] G. Aad *et al.* (ATLAS Collaboration), Phys. Rev. D **90**, 052005 (2014).
[65] V. Khachatryan *et al.* (CMS Collaboration), J. High Energy Phys. 04 (2015) 025.
[66] ATLAS Collaboration, Report No. ATLAS-CONF-2012-153.
[67] T. Aaltonen *et al.* (CDF Collaboration), Phys. Rev. Lett. **102**, 091805 (2009).
[68] T. Aaltonen *et al.* (CDF Collaboration), Phys. Rev. Lett. **106**, 121801 (2011).
[69] G. Aad *et al.* (ATLAS Collaboration), J. High Energy Phys. 03 (2015) 041.
[70] G. Aad *et al.* (ATLAS Collaboration), Phys. Rev. Lett. **115**, 031801 (2015).
[71] CMS Collaboration, Report No. CMS-PAS-SUS-12-027.
[72] S. Chatrchyan *et al.* (CMS Collaboration), Phys. Rev. Lett. **111**, 221801 (2013).
[73] T. Aaltonen *et al.* (CDF Collaboration), Phys. Rev. Lett. **105**, 191801 (2010).
[74] J. Alwall, R. Frederix, S. Frixione, V. Hirschi, F. Maltoni, O. Mattelaer, H.-S. Shao, T. Stelzer, P. Torrielli, and M. Zaro, J. High Energy Phys. 07 (2014) 079.
[75] T. Sjostrand, S. Mrenna, and P. Z. Skands, J. High Energy Phys. 05 (2006) 026].
[76] J. Pumplin, D. R. Stump, J. Huston, H. L. Lai, P. M. Nadolsky, and W. K. Tung, J. High Energy Phys. 07 (2002) 012.
[77] M. Cacciari, G. P. Salam, and G. Soyez, Eur. Phys. J. C **72**, 1896 (2012).
[78] W. Beenakker, R. Hopker, and M. Spira, arXiv:hep-ph/9611232.
[79] SM Higgs production cross sections at $\sqrt{s} = 13$–14 TeV.
[80] J. Baglio, L. D. Ninh, and M. M. Weber, arXiv:1310.3972.